Langevin approach to magnetic-field-gradient-induced spin relaxation in a coated cell

Junhe Zheng, Wei Xiao, Sheng Li, Xiang Peng, Teng Wu,* and Hong Guo†
School of Electronics, Peking University, Beijing 100871, China
and Center for Quantum Information Technology, Peking University, Beijing 100871, China

(Received 3 July 2023; revised 25 December 2023; accepted 4 January 2024; published 7 February 2024)

Magnetic-field-gradient-induced spin polarization transverse relaxation is re-examined in an alkali-metal atomic cell with antirelaxation coating. The experimentally observed motional-narrowing effect in a paraffin-coated vapor cell, a phenomenon for depicting the suppression of spin polarization transverse relaxation caused by the magnetic-field gradient, is more than an order of magnitude weaker than theoretical predictions. Such a discrepancy is due to the existence of background gas. By taking the background gas into consideration, Redfield theory combined with the Langevin approach is proposed to depict the magnetic-field-gradient-induced spin relaxation in a coated cell, and the model is verified to be consistent with the previous results derived under two limits in which the mean free path is either much smaller (diffusion regime) or much larger than (ballistic regime) the cell size. Our work provides a potentially feasible method to evaluate the background gas pressure inside the coated cell, and it can help to foster better comprehension of the performance of an antirelaxation coated cell.

DOI: 10.1103/PhysRevA.109.022803

I. INTRODUCTION

An atomic vapor cell with antirelaxation coating has found tremendous applications in magnetometry [1–3], spin noise measurement [4–6], frequency standards [7–10], and fundamental physics experiments [11–13]. Considering that the atoms in the coated cell can experience thousands of collisions with the cell wall without losing polarization [14,15], and taking into account the low saturated atomic vapor pressure, atoms move rapidly within the cell. The rapid atomic motion brings many benefits, such as the motional-narrowing effect [16], which suppresses the spin polarization transverse relaxation caused by the magnetic-field gradient. The coated cell, typically the one filled with alkali-metal atoms, is widely used for measuring Earth's magnetic field [17,18], and it has the potential to achieve femtotesla sensitivity even in a magnetically unshielded environment [19].

A persistent goal has been learning how to precisely and quantitatively model the spin relaxation mechanism under the influence of a magnetic-field gradient. In the majority of previous work for this topic, a diffusion equation has been used to describe the motion of spin polarization [20–24], which is applicable for a liquid NMR sample [25,26] or an atomic vapor cell filled with high-pressure gas (the pressure is typically larger than 10^4 Pa) [27,28]. Under this condition, the mean free path of atoms, i.e., λ, characterizing the average distance over which a moving atom travels before collisions with other atoms, is on the order of $\sim\mu$m or less and is typically much smaller than the cell size, i.e., R. The diffusion equation is valid under the condition in which $\lambda \ll R$ [29], i.e., the diffusion regime.

Nevertheless, without buffer gas, the mean free path of the atoms in a well-performed coated cell is normally on the order of hundreds of meters, and the atoms may travel *ballistically* between collisions with the cell wall, i.e., the ballistic regime. The diffusion equation is thus invalid for describing the atomic motion within the coated cell. To solve this problem, Ref. [30] presents a neat and clever approach, i.e., it analyzes the accumulation of a random phase, and in turn it gives a quantitative expression of the relation between the magnetic-field gradient and spin polarization relaxation in the coated cell.

Besides of the two cases mentioned above, i.e., when the atomic mean free path is much smaller (*diffusion regime*) or larger than (*ballistic regime*) the size of the vapor cell, it is natural to ask (i) if there exists an *intermediate regime*, in which the mean free path is comparable with the size of the atomic vapor cell, i.e., on the order of millimeters or centimeters, and (ii) if so, which theoretical model is suitable to depict the magnetic-field-gradient-induced spin polarization relaxation?

For the first question, the mean free path of the atoms in the coated cell could be suppressed from hundreds of meters to millimeters. The dominant factor is due to the amount of background gas occurring inside the coated cell. The background gas could be typically generated from two processes, i.e., the out-gassing of the chemical reactions between the alkali-metal atoms and the paraffin coating [31,32], and the heating process, such as ripening [33,34]. The occurrence of the background gas inside the coated cell has been proved experimentally [35–37], while it is normally taken as a neglected factor for analyzing the spin polarization relaxation, especially under a magnetic-field gradient, since the pressure of the emerging background gas ($\sim$1 Pa) is much smaller than the pressure of the buffer gas added inside the cell [38]. Accordingly, the coated cell with background gas is different from the case in which the coated cell is filled with buffer gas, under which the diffusion equation is applicable to analyze the atomic motion [39]. However, the pressure of background gas is much larger than the saturated vapor pressure of the

*Corresponding author: wuteng@pku.edu.cn
†Corresponding author: hongguo@pku.edu.cn

alkali-metal atoms ($\sim 10^{-5}$ Pa), and it makes the motional characteristics of atoms inside the coated cell distinct from the ballistic case.

For the second question, previous theoretical models for the diffusion regime and the ballistic regime are not suitable for characterizing the magnetic-field-gradient-induced spin relaxation in a coated cell with background gas, which is in the intermediate regime and has attracted increasing attention, especially on how to develop a generalized theoretical model to cover the full range of the mean free path. In general, the Redfield theory is widely used to solve this problem, together with various other developed approaches to calculate the autocorrelation function or power spectral density of the fluctuating field experienced by moving spin polarization [40–48].

One way to obtain the power spectral density of the fluctuating field for all values of the mean free path is based on the velocity autocorrelation of spin polarization. The authors analyze the trajectory and velocity of a particle and develop a damped oscillation equation to characterize the velocity autocorrelation [40]. This method is then applied in Ref. [41], and different angular distributions of the trajectory need to be considered for different boundary shapes. To simplify the calculation, the correlation function and power spectral density are calculated in rectangular boundary, with a single angle of trajectory, and the derived results are consistent with previous work in the diffusion regime.

Telegrapher's equation is introduced in Ref. [42] to obtain the conditional probability of a particle's position, so as to describe the atomic motion for one-dimensional motion with a plane boundary. The validity of this model is verified under different mean free paths through Monte Carlo simulations. However, the solutions of the two- or three-dimensional telegrapher's equation cannot characterize the corresponding conditional probability since they can be negative values [43]. To solve this problem, the approach based on persistent continuous-time random walks [44] is applied in Ref. [45] to calculate the power spectral density in the one-, two-, and three-dimensional atomic motion. The corresponding method is extended by considering the velocity distribution of the scattered particles in Ref. [46]. Besides, there exist other investigations on extending the power spectral density by applying a succession of integrations by parts, and we expect that the results are valid from the diffusion regime to the ballistic regime, which can be seen in Refs. [47,48].

In this manuscript, we present a complementary theoretical model, which combines the Redfield theory with Langevin's diffusion approach to deal with the magnetic-field-gradient-induced spin relaxation covering a full range of the mean free path in the coated cell. The results of our model are verified to be consistent with the established results derived under two extreme conditions, i.e., the diffusion regime and the ballistic regime.

II. THEORETICAL MODEL

This section introduces the details of our proposed theoretical model based on the Redfield theory combined with Langevin's diffusion approach. Our model takes the different regimes, or equivalently, the mean free paths (see Appendix A for detailed clarifications), into consideration, i.e., the mean free path is larger than, comparable to, or smaller than the vapor cell.

A. Redfield theory with Langevin's diffusion model

In this paper, Redfield theory, which is a generalized treatment of second-order time-dependent perturbation [49], is applied to analyze the magnetic-field-gradient-induced spin relaxation in coated cells. Redfield theory is valid under the following two approximations [50]: (i) Weak-coupling approximation: the physical system is weakly coupled with the environment, i.e., the perturbation caused by the environment on the system is small; (ii) Markov approximation: the perturbation caused by the environment on the system is a memoryless process, indicating that the evolution of the system over time is independent of the previous state. For the coated cell, perturbation caused by the magnetic-field gradient is considerably smaller compared to that by the static bias field in most application scenarios. Besides, the random motion of atoms in the coated cell makes the magnetic-field-gradient-induced perturbation a random process. Thus, both of the aforementioned two approximations are satisfied for the coated vapor cell.

With the presence of the magnetic-field gradient, the static bias magnetic field $B_0\vec{e}_z$ should be replaced with $B_0\vec{e}_z + \vec{B}_1$. For simplicity, the influence of a first-order magnetic-field gradient can be written as $\vec{B}_1(\vec{r})$, which is a static magnetic field that varies with space. Here, the variation of the magnetic-field gradient over time is not considered. However, due to the rapid movement of the atom within the cell, the atom encounters varying magnetic fields at different moments. As a consequence, for a specific atom, the magnetic field it experiences varies with time and has the form $\vec{B}_1(\vec{r}, t)$ or $\vec{B}_1(\vec{r}(t))$. The impact of the magnetic-field gradient on the evolution of atomic spin can be regarded as a perturbation under the condition of $|\vec{B}_1(\vec{r}, t)| \ll B_0$. Based on the Redfield theory [16,49], the relaxation of spin polarization can be depicted by the power spectral density of the magnetic-field perturbation, and the relaxation times T_1 and T_2, which characterize the decay of longitudinal and transverse polarization over time, take the forms

$$\frac{1}{T_1} = \frac{\gamma^2}{2}[S_{1x}(\omega_0) + S_{1y}(\omega_0)],$$
$$\frac{1}{T_2} = \frac{1}{2T_1} + \frac{\gamma^2}{2}S_{1z}(0), \tag{1}$$

where

$$S_{1x,y,z}(\omega) = \int_{-\infty}^{\infty} \langle B_{1x,y,z}(\vec{r}, t) B_{1x,y,z}(\vec{r}, t+\tau)\rangle e^{-i\omega\tau} d\tau \tag{2}$$

are the power spectral density of magnetic-field perturbations in the x, y, z directions, respectively. $\langle \cdots \rangle$ means the ensemble average, γ is the gyromagnetic ratio, and $\omega_0 = \gamma B_0$ is the atomic spin precession frequency under the influence of the bias magnetic field B_0.

Considering the existence of the static bias field $B_0\vec{e}_z$, Eq. (1) can be phenomenologically analyzed in the frame rotating at the Larmor frequency ω_0. T_1 characterizes the decay of longitudinal spin polarization, and such a decay is caused

by static transverse magnetic fields B_{1x} and B_{1y} in the rotating frame. The static fields B_{1x} and B_{1y} in the rotating frame oscillate at Larmor frequency ω_0 in the laboratory frame. That is why T_1 is related to $S_{1x}(\omega_0)$ and $S_{1y}(\omega_0)$. On the other hand, T_2 characterizes the decay of transverse spin polarization and is related to the linewidth of the magnetic resonance signal (see Appendix B), and such a decay is caused by static longitudinal magnetic field B_{1z} in the rotating frame. Static fields B_{1z} in the rotating frame are also static in the laboratory frame. That is why T_2 is related to $S_{1z}(0)$.

To derive the form of the spin relaxation, it is necessary to calculate the autocorrelation function of perturbation caused by the magnetic-field gradient, i.e., $\langle B_{1i}(t)B_{1i}(t+\tau)\rangle$, which can be represented by $|\nabla B_{1i}|^2$ times the autocorrelation function of the position $\langle i(t)i(t+\tau)\rangle$, and it has the from

$$\langle B_{1i}(t)B_{1i}(t+\tau)\rangle = |\nabla B_{1i}|^2\langle i(t)i(t+\tau)\rangle, \tag{3}$$

where $i = x, y, z$. If the static bias field B_0 is large enough, i.e., $\omega_0 \gg 1/\tau_R$ or D/R^2, where $\tau_R = 4R/3\bar{v}$ is the average time between consecutive atom-wall collisions, R is the radius of the cell, $\bar{v}$ is the thermal velocity of atoms, and D is diffusion coefficient of atoms, then the impact of T_1 on T_2 can be ignored (see Appendix C). Under this condition, magnetic-field-gradient-induced transverse relaxation has the form

$$\begin{aligned}\frac{1}{T_2} &= \frac{\gamma^2}{2}S_{1z}(0)\\ &= \frac{\gamma^2}{2}|\nabla B_{1z}|^2\int_{-\infty}^{\infty}\langle z(t)z(t+\tau)\rangle d\tau,\end{aligned} \tag{4}$$

and $\langle z(t)z(t+\tau)\rangle$, which is the autocorrelation function of the position along the z direction and is assumed to be a stationary process, is given by conditional probability density, which depicts the characteristics of atomic motion,

$$\begin{aligned}\langle z(t)z(t+\tau)\rangle &= \langle z(t_0+\tau)z(t_0)\rangle\\ &= \iint \rho(\vec{r}_0,t_0)\rho(\vec{r},t_0+\tau\mid\vec{r}_0,t_0)zz_0\,d\Omega d\Omega_0,\end{aligned} \tag{5}$$

where

$$d\Omega = r^2\sin\theta dr d\theta d\phi, \quad d\Omega_0 = r_0^2\sin\theta_0 dr_0 d\theta_0 d\phi_0, \tag{6}$$

$z(t_0+\tau) = z$, $z(t_0) = z_0$, and $\rho(\vec{r}_0,t_0)$ is a uniform initial probability density in a spherical cell with radius R and volume V,

$$\rho(\vec{r}_0,t_0) = \frac{1}{V} = \left(\frac{4\pi R^3}{3}\right)^{-1}. \tag{7}$$

$\rho(\vec{r},t\mid\vec{r}_0,t_0)$ in Eq. (5) is the conditional probability density of an atom at position $\vec{r}$ at time t, if t_0 and $\vec{r}_0$ are the initial time and position. The theoretical model that we develop is applicable for different cell shapes, taking different boundary conditions into consideration.

Reviewing the above procedures, magnetic-field-gradient-induced spin relaxation can be derived based on the following three steps:

(i) Calculate $\rho(\vec{r},t\mid\vec{r}_0,t_0)$ through the theoretical analysis of the atomic motion, and calculate $\langle z(t)z(t+\tau)\rangle$ with Eq. (5).

(ii) Calculate $\langle B_{1z}(t)B_{1z}(t+\tau)\rangle$ based on the form of $\langle z(t)z(t+\tau)\rangle$ by using Eq. (3).

(iii) Calculate transverse relaxation time T_2 based on the form of $\langle B_{1z}(t)B_{1z}(t+\tau)\rangle$ through Eq. (4).

The first step plays a key role in deriving the calculation. It is significant to choose a reasonable model to describe the motional characteristics of atoms in the coated cell. The corresponding theory applied to describe the atomic motion in most previous work is based on Einstein's work for Brownian motion [29], and it is known as Torrey's diffusion equation for analyzing the spin relaxation caused by an inhomogeneous magnetic field [20–22]. This model is valid *only if* the mean free path of the concerned particle is much smaller than the size of the boundary [29,41], e.g., the cell with high-pressure buffer gas, which is not the case for the antirelaxation coated vapor cell, since the pressure of the background gas within the coated cell is several orders of magnitude smaller than the pressure of the buffer gas.

Langevin's diffusion model is used for analyzing the Brownian motion, which focuses on the velocity of Brownian motion particles. The restriction on Torrey's diffusion model ($\lambda \ll R$) does not exist in Langevin's diffusion model [29], which covers from the ordinary ballistic motion model to Einstein's (Torrey's) diffusion model [29,51]. For this reason, Langevin's diffusion model is a more general diffusion model to analyze the random motion of particles, especially for describing the motion of atoms in the coated cell, in which the mean free path of the atoms is comparable with the size of the coated cell, i.e., on the order of millimeters or centimeters. Relevant work can be seen in Ref. [5], in which Langevin's diffusion model with ideal coating as the boundary condition is applied to describe the two-dimensional atomic motion within an OTS-coated Rb vapor cell, and to analyze the corresponding spin-noise spectrum of hot vapor atoms.

Based on the above considerations, Langevin's diffusion model is used for calculating $\rho(\vec{r},t\mid\vec{r}_0,t_0)$ in our work to describe atomic motion within the coated cell. According to Langevin's diffusion model shown in Appendix D, for the motion of atoms in a coated cell, $\rho(\vec{r},t\mid\vec{r}_0,t_0)$ obeys the following equation:

$$\frac{\partial}{\partial t}\rho(\vec{r},t\mid\vec{r}_0,t_0) = D\left(1-e^{-\frac{|t-t_0|}{\tau_D}}\right)\nabla^2\rho(\vec{r},t\mid\vec{r}_0,t_0), \tag{8}$$

where D is the diffusion coefficient of atoms within the coated cell. $\tau_D = Dm/(k_{\mathrm{B}}T)$, in which m is the mass of a single atom, T is the temperature of the cell, and k_{B} is the Boltzmann constant. The boundary condition for Eq. (8) has the form

$$\vec{n}\left.\frac{\partial\rho(\vec{r},t\mid\vec{r}_0,t_0)}{\partial n}\right|_{r=R} = 0, \tag{9}$$

where $\vec{n}$ is an outwardly directed normal unit vector to the spherical wall. Equation (9) is called the Neumann boundary condition [52,53], typically for the cases in which the wall-induced relaxation time is much longer than the atomic motional time between adjacent wall collisions, as shown in Appendix E. Accordingly, the Neumann boundary condition is suitable for ideal coating, which assumes that the impact of wall-collision-induced relaxation is neglected. Based on this

consideration, the corresponding initial condition is

$$\rho(\vec{r}, t \mid \vec{r}_0, t_0) = \delta(\vec{r} - \vec{r}_0) = \frac{1}{r^2 \sin\theta}\delta(r - r_0)\delta(\theta - \theta_0)\delta(\phi - \phi_0), \quad (10)$$

which describes a single atom at initial position $\vec{r}_0$ with initial time t_0. Combining Eqs. (8)–(10), the general solution of the diffusion equation takes the form

$$\rho(\vec{r}, t \mid \vec{r}_0, t_0) = \frac{1}{R^3}\sum_{n,l,m} A_{ln} j_l\left(\frac{k_{ln} r}{R}\right) j_l\left(\frac{k_{ln} r_0}{R}\right) Y^*_{lm}(\theta, \phi) Y_{lm}(\theta_0, \phi_0) \exp\frac{-k_{ln}^2 D\left[|t - t_0| + \tau_D\left(e^{\frac{-|t-t_0|}{\tau_D}} - 1\right)\right]}{R^2}, \quad (11)$$

where $Y_{lm}(\theta, \phi)$ is the spherical harmonic, with l and m as the two variables, $j_l(k)$ is the spherical Bessel function, and k_{ln} is the nth zero of $dj_l(k)/dk$. The normalization constant A_{ln} satisfies

$$A_{ln} = R^3\left[\int_0^R r^2 j_l^2\left(\frac{k_{ln} r}{R}\right) dr\right]^{-1}. \quad (12)$$

Based on these, the autocorrelation function of position $\langle z(t + \tau)z(t)\rangle$ can be calculated. Substituting Eq. (11) into Eq. (5), it can be found after some algebra that

$$\langle z(t + \tau)z(t)\rangle = R^2 \sum_n A_{1n} C_n F_n, \quad (13)$$

where

$$C_n = \frac{1}{R^8}\left[\int_0^R r^3 j_1\left(\frac{k_{1n} r}{R}\right) dr\right]^2 \quad (14)$$

and

$$F_n = \exp\frac{-k_{1n}^2 D\left[|t - t_0| + \tau_D\left(e^{\frac{-|t-t_0|}{\tau_D}} - 1\right)\right]}{R^2}. \quad (15)$$

Combining Eqs. (4), (13), and (B4) (listed in Appendix B), the broadening of the magnetic resonance linewidth caused by the magnetic-field gradient takes the form

$$\frac{1}{\pi T_2} = \frac{\gamma^2}{2\pi} S_{1z}(0) = \frac{\gamma^2 |\nabla B_{1z}|^2}{2\pi}\int_{-\infty}^{+\infty} \langle z(t + \tau)z(t)\rangle d\tau \approx \frac{\gamma^2}{\pi}\left(\frac{\partial B_{1z}}{\partial z}\right)^2 R^2 \sum_n A_{1n} C_n \int_0^{+\infty} F_n d\tau. \quad (16)$$

Here we assume that $\partial B_{1z}/\partial z$ is the main component of the axial gradient ∇B_{1z}. It can be seen from Eq. (16) that the transverse relaxation has a quadratic relation with the first-order axial magnetic-field gradient, which agrees well with previous theoretical models. In addition to the quadratic relation, our purpose is to derive an accurate form of the axial quadratic coefficient a_z, which has the form

$$a_z = \frac{\gamma^2}{\pi} R^2 \sum_n A_{1n} C_n \int_0^{+\infty} F_n d\tau. \quad (17)$$

In the following subsections, we compare our model shown in Eq. (16) with previous work under two extreme conditions, i.e., when the mean free path is much smaller or larger than the atomic vapor cell.

B. Langevin's diffusion model for $\lambda \gg R$

When the mean free path of atoms is much larger than the cell size ($\lambda \gg R$), which means that the presence of background gas can be neglected in the coated cell and only the saturated vapor pressure of atoms is taken into consideration, the average time between consecutive atom-wall collisions ($\sim R/\bar{v}$) is much smaller than the average time between consecutive atom-atom collisions ($\sim\lambda/\bar{v}$). At this time, atomic motion between adjacent wall collisions described by Langevin's diffusion model is in an approximate straight line, i.e., ballistic motion [29]. It is derived that (the relation between the diffusion coefficient and the mean free path can be found in Appendix A)

$$\int_0^{+\infty} \exp\frac{-k_{1n}^2 D\left[|t - t_0| + \tau_D\left(e^{\frac{-|t-t_0|}{\tau_D}} - 1\right)\right]}{R^2} d\tau \approx \int_0^{+\infty} \exp\frac{-k_{1n}^2\left(\frac{k_B T}{2m}\right)|t - t_0|^2}{R^2} d\tau = \frac{R}{k_{1n}}\sqrt{\frac{m\pi}{2k_B T}}. \quad (18)$$

Under this condition, by using Eq. (16), the spin relaxation caused by the magnetic-field gradient is

$$\frac{1}{\pi T_2} = \frac{\gamma^2}{\pi}\left(\frac{\partial B_{1z}}{\partial z}\right)^2 R^2 \sum_n A_{1n} C_n \int_0^{+\infty} F_n d\tau = \frac{\gamma^2}{\pi}\left(\frac{\partial B_{1z}}{\partial z}\right)^2 R^2 \sum_n A_{1n} C_n \frac{R}{k_{1n}}\sqrt{\frac{m\pi}{2k_B T}} \approx 0.066\frac{\gamma^2 R^3}{\bar{v}}\left(\frac{\partial B_{1z}}{\partial z}\right)^2. \quad (19)$$

Reference [30] proposed a theoretical model based on the phase accumulation method to describe the influence of a magnetic-field gradient on a coated alkali atomic cell. The quadratic relation between the linewidth of magnetic resonance and the magnetic-field gradient has the form

$$\frac{1}{\pi T_2} \approx 0.042\frac{\gamma^2 R^3}{\bar{v}}\left(\frac{\partial B_i}{\partial x_i}\right)^2, \quad (20)$$

where γ is the gyromagnetic ratio, R is the radius of the cell, $\bar{v}$ is the atomic thermal velocity, and $\partial B_i/\partial x_i$ is the magnetic-field gradient along the x_i direction.

Comparing Eqs. (19) and (20), it can be found that Langevin's diffusion model under $\lambda \gg R$ has the same form

as that of the phase accumulation model,

$$\frac{1}{\pi T_2} \sim k\frac{\gamma^2 R^3}{\bar{v}}\left(\frac{\partial B_i}{\partial x_i}\right)^2. \tag{21}$$

Therefore, when the mean free path of atoms is much larger than the radius of the coated cell, Langevin's diffusion model turns into ballistic motion. We notice that there exists some difference between the coefficient k of the two models shown in Eqs. (19) and (20). Such a difference could be attributed to the assumptions and approximations of the two models. For instance, in Ref. [30], i.e., the phase accumulation model for the ballistic regime, magnetic-field gradient information is replaced by a typical constant value to simplify the calculation, and a characteristic relaxation is assumed to happen when the total accumulated phase is equal to $\sqrt{2}$, which are not needed in our Langevin diffusion model. Furthermore, the Neumann boundary condition of our model shown in Eq. (9) is crude for characterizing the nature of atom-wall collisions in the ballistic regime. The specific form of reflections (diffuse or specular) can affect the calculations and thus the magnetic-field-gradient-induced relaxation [54].

C. Langevin's diffusion model for $\lambda \ll R$

When the pressure in the cell is too high for atoms to travel ballistically between the wall, e.g., when the cell is filled with buffer gas, the mean free path of the atom is significantly suppressed and is much smaller than the size of the coated cell ($\lambda \ll R$). Under this condition,

$$\begin{aligned} F_n &= \exp\frac{-k_{1n}^2 D\left[|t-t_0| + \tau_D\left(e^{\frac{-|t-t_0|}{\tau_D}} - 1\right)\right]}{R^2} \\ &\approx \exp\frac{-k_{1n}^2 D|t-t_0|}{R^2}, \end{aligned} \tag{22}$$

and the spin relaxation caused by the magnetic-field gradient under this condition is

$$\begin{aligned} \frac{1}{\pi T_2} &= \frac{\gamma^2}{\pi}\left(\frac{\partial B_{1z}}{\partial z}\right)^2 R^2 \sum_n A_{1n} C_n \int_0^{+\infty} F_n d\tau \\ &= \frac{8\gamma^2 R^4}{175\pi D}\left(\frac{\partial B_{1z}}{\partial z}\right)^2. \end{aligned} \tag{23}$$

This expression of T_2 is consistent with Eq. (C4) in Appendix C, which is based on Torrey's diffusion model [22,23] and is quite different from Eq. (20) for ballistic motion.

The differences between the two diffusion models. i.e., Torrey's diffusion model and Langevin's diffusion model, are summarized in Fig. 1. The ratios of the axial quadratic coefficients a_z corresponding to these two models are calculated for the potassium atomic coated cell with $R = 2$ cm, under different mean free paths. It is shown that, when the mean free path is small, i.e., less than ~1 mm, the results calculated by the two methods are almost identical (the ratio is ~1), indicating the consistency between the two models. When the mean free path becomes larger, the deviation between the axial quadratic coefficients a_z calculated by the two diffusion models becomes deviated from 1, indicating that Torrey's diffusion model could underestimate the spin transverse relaxation effect caused by the magnetic-field gradient.

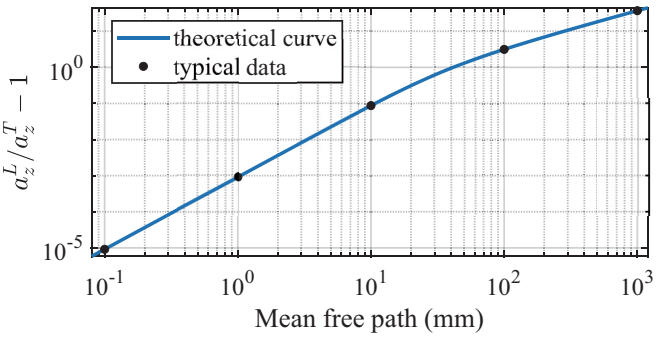

FIG. 1. Ratios of the axial quadratic coefficients corresponding to the proposed theoretical model based on Langevin's diffusion model a_z^L and the previous theoretical model based on Torrey's diffusion model a_z^T, under the conditions of the mean free paths varying from 0.1 to 1000 mm. The blue line denotes the theoretical curve, and the black points are the calculated results at some particular values of the mean free paths. The radius of a cell is set to $R = 2$ cm, and the cell is filled with potassium atoms at $T = 50\,^\circ$C.

In conclusion, Torrey's diffusion model and the phase accumulation mode for ballistic motion can be approximated as two extreme cases of our proposed Langevin model under $\lambda \ll R$ and $\lambda \gg R$. Langevin's diffusion model is thus suitable to describe the atomic motion in the coated cell under different conditions, i.e., with or without background gas.

III. EXPERIMENT AND ANALYSIS

This section introduces an illustrative example of the impact of background gas on magnetic-field-gradient-induced relaxation within the coated cell. For the coated cell that we use, the magnetic-field-gradient-induced spin relaxation is over an order of magnitude larger than the predicted value based on the theoretical model, which is suitable in the ballistic regime. Such a finding motivates us to think that there might exist some additional gas component inside the coated vapor cell. In addition, we also consider factors such as those from the coating absorption, the light-induced desorption, and the atomic transit effect, which may affect the spin relaxation caused by the magnetic-field gradient.

A. Magnetic-field-gradient-induced spin relaxation

We use a prototype atomic magnetometer under a conventional optical-magneto double resonance configuration [55,70] (see Appendix B), which provides a convenient method to measure the spin relaxation effect caused by the magnetic-field gradient. A brief configuration of the magnetometer is shown in Fig. 2(a). The core element is an antirelaxation paraffin-coated cell filled with potassium atoms. To simplify the analysis, we use a spherical-shaped vapor cell, with a radius of 2 cm, to perform our measurement. The vapor cell is heated and kept at a temperature of 50 °C to improve the signal-to-noise ratio, under which the paraffin coating can be well preserved. A circularly polarized pump light, which is tuned to be resonant with the potassium D1 line, is used to optically pump the atomic spin along the direction of the static bias field B_0. An oscillating magnetic field is

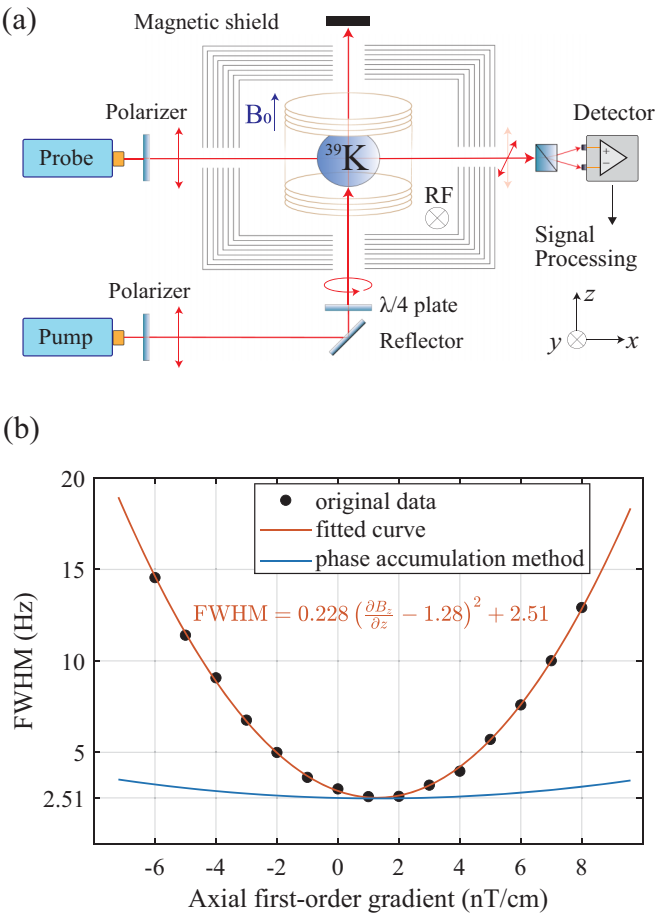

FIG. 2. (a) Experimental configuration of the atomic magnetometer for measuring the magnetic-field-gradient-induced spin relaxation. (b) Relation between the measured linewidth (FWHM, full width at half-maximum, black dots) of the magnetic resonance signal and the first-order magnetic-field gradient, $(\partial B_z/\partial z)$, under $B_0 \approx 900$ nT. A quadratic function (red line) is used to fit the measured data with quadratic coefficient $a_z \approx 0.228$, and the residual magnetic field gradient is 1.28 nT/cm. The blue line is the theoretically predicted linewidth based on the phase accumulation method with a quadratic coefficient $a_z \approx 0.0143$.

applied along the transverse direction to drive the atomic spin precession synchronously if the oscillation frequency is equal to the precession frequency. Thus, a maximum macroscopic transverse spin polarization is generated. A linearly polarized laser light (∼hundreds of MHz detuned from the D2 line) propagating along the transverse direction is used to measure the generated spin polarization through the optical rotation effect.

We apply an anti-Helmholtz coil to generate different axial magnetic-field gradients $\partial B_{1z}/\partial z$ to the atomic magnetometer, and we record the linewidths of magnetic resonances under different magnetic-field gradients in order to obtain a quantitative relation between the spin relaxation and the magnetic-field gradient. It should be emphasized that the experiment is not intentionally arranged, and the conclusion derived in this work is general for experiments concerning the magnetic-field-gradient-induced spin relaxation.

In addition to the quadratic relation between the signal linewidth and the magnetic-field gradient, we further compare the theoretically predicted quadratic coefficient a_z based on the phase-accumulation model shown in Ref. [30] with the experimental measurement. There exists over an order of magnitude difference between the two results; see Fig. 2(b). One of the advantages of the coated cell is the suppression of the magnetic-field-gradient-induced spin relaxation, or the motional narrowing effect. However, for the coated cell that we use, the motional narrowing effect is highly suppressed. It has been demonstrated experimentally that the dominant factor originates from a tiny amount of background gas [37,38], which makes the motion of the atoms distinct from the ballistic mode without background gas.

To match the experimental results about the axial quadratic coefficient a_z recorded in Fig. 2(b), which takes the form (see Appendix B)

$$a_z = \frac{1}{\pi T_2}\left(\frac{\partial B_{1z}}{\partial z}\right)^{-2} \approx 0.228\left(\mathrm{Hz}\frac{\mathrm{cm}^2}{\mathrm{nT}^2}\right), \tag{24}$$

we combine Eqs. (17) and (24) and we derive the value of the diffusion coefficient D and mean free path λ by using our proposed model,

$$D = \frac{\bar{v}\lambda}{6} \approx 0.2\,\mathrm{m}^2/\mathrm{s}, \quad \lambda \approx 2.63\,\mathrm{mm}, \tag{25}$$

where $\bar{v} = 453$ m/s is the thermal velocity. The results indicate that the mean free path of the alkali atoms in the coated cell that we use is suppressed, from the order of hundreds of meters with saturated vapor pressure, to millimeters, which verifies the existence of the background gas. Such a finding provides a convenient way to determine if there exists any background gas inside the coated cell without breaking the cell through monitoring the dependence of the magnetic resonance signal linewidth with different magnetic field gradients. Besides, the mean free path that we derive is of the same order of magnitude as the value ($\lambda = 1.4$ mm) deduced by Refs. [37,38], indicating that the emergence of background gas is not an occasional phenomenon for the coated cell.

B. Potential relaxation mechanisms

Our theoretical model for depicting the magnetic-field-gradient-induced spin relaxation is based on the analysis of the atomic motion. In addition to the background gas or the buffer gas, there are some other factors that could alter the atomic motional characteristics and should be taken into consideration as well.

1. Coating absorption effect

The spin relaxation caused by interaction between alkali-metal atoms and the coating, as well as the physical mechanism of the coating, are relatively complex issues [56–59] and are still under investigation. When the alkali atoms collide with the coated wall, atoms could be absorbed by the coating without being relaxed. Such a phenomenon may affect the atomic motion inside the coated cell, and it depends on the average dwell time τ_s of the atoms. Here, τ_s reflects quantitatively how long the spin-polarized atom is trapped in the coating without losing polarization [59].

Taking the dwell time into consideration, the boundary condition of our proposed model, i.e., Eq. (9), should be modified accordingly as [57,59]

$$\vec{n}\,\frac{\partial\rho(\vec{r},t\mid\vec{r}_0,t_0)}{\partial n}\bigg|_{r=R}\approx-\vec{n}\frac{\tau_s\bar{v}}{4}\,\frac{\partial^2\rho(\vec{r},t\mid\vec{r}_0,t_0)}{\partial n^2}\bigg|_{r=R}, \quad (26)$$

where $\bar{v}$ means the atomic thermal velocity. Precise measurement about the dwell time of the coating still remains difficult [58,60,61]. In terms of the potassium atomic cell coated with paraffin that we use, τ_s is assumed to be 1 ns $\sim$ 1 μs. Since $\tau_s\bar{v}\ll 1$, the right part of Eq. (26) is approximated to be zero, indicating that the absorption of atoms by the coating has a negligible impact on the magnetic-field-gradient-induced spin relaxation.

2. LIAD effect

The light-induced atomic desorption (LIAD) effect happens when the coated cell is exposed to a laser with a sufficiently shorter wavelength than the resonant wavelength and high enough power (on the order of several hundreds of milliwatts). Under this condition, alkali atoms are desorbed from the cell wall, and the atomic density inside the coated cell becomes increased [62–65], which alters the motional characteristics of the atoms inside the cell. Considering the experimental systems for obtaining magnetic resonance, the power of the laser is usually on the order of milliwatts, and the detuning of the laser frequency is on the order of hundreds of MHz. Taking our prototype atomic magnetometer as an example, the power of both lasers is less than 1 mW to avoid the power broadening effect, and the detuning of nonresonant probe light is ∼200 MHz, which hardly meets the basic requirements of the LIAD effect [63,65]. Besides, even if the LIAD effect exists, we prove that as long as the increase of atomic density in the cell is less than two orders of magnitude (which rarely happens under the influence of the LIAD effect), the proposed theoretical model for calculating the magnetic-field-gradient-induced spin relaxation is still valid, and the LIAD effect could be neglected.

3. Atomic transit effect

The size of the laser beam determines the transit time at which atoms pass through the beam region [66–68]. For the coated cell, even in the presence of background gas (∼Pa), the atom passes through the beam region multiple times during one pump period ($\sim 10^{-1}$ s). Then the laser beam interacts with the atomic ensemble in the entire coated cell, not just atoms within the beam region. Under this condition, the influence of the transit effect, which is decided by the size of the beam, is negligible when we consider the spin relaxation effect caused by the magnetic-field gradient in the coated cell.

In terms of the cell with high pressure, i.e., atomic motion is highly constrained within a small region, the distance of atomic diffusion during one pump period may be smaller than the size of the cell. Accordingly, the transit effect should not be ignored at this time. Under this condition, in order to study the spin relaxation of the atomic ensemble within the entire cell, as analyzed in our theory, the size of the beam should be larger than the size of the cell to ensure that the cell is fully covered.

IV. DISCUSSION

A. Evaluation of background gas pressure

Our work provides a potentially promising method to estimate the pressure of the background gas within the coated cell. Magnetic-field-gradient-induced spin relaxation is related to the mean free path of atoms in the coated cell, and the mean free path λ is determined by the pressure of the background gas. As a consequence, the pressure of the background gas in the coated cell could be estimated through the following steps:

(i) Apply different imposed axial magnetic-field gradients $\partial B_z/\partial z$ to the coated cell, and measure the corresponding linewidths of magnetic resonances.

(ii) Fit the relation between linewidths and $\partial B_z/\partial z$ with a quadratic function, and then record the fitted quadratic coefficient a_z.

(iii) Derive the relation between a_z and diffusion coefficient D based on theoretical analysis about atomic motion in the coated cell.

(iv) Combine the experimental fitted a_z and theoretical analysis, and calculate the diffusion coefficient D.

(v) Derive the corresponding mean free path of alkali atoms λ through the diffusion coefficient D.

(vi) Obtain the pressure of background gas p_b through the mean free path λ.

Taking the measured axial quadratic coefficient $a_z\approx 0.228$ in our experiment as an example, the corresponding diffusion coefficient D and the mean free path λ can be solved numerically. The mean free path λ of the atoms in the coated cell is estimated to be 2.63 mm, and it is related to the pressure of the background gas,

$$\lambda = k_\mathrm{B}T/(p_\mathrm{b}\sigma_\mathrm{c}), \quad (27)$$

where p_b is the pressure of the background gas in the coated cell, and σ_c is the cross section of the collisions between potassium atoms and the background gas inside the coated cell. Thus, based on Eq. (27), an accurate estimation of the background gas pressure requires an accurate value of the cross section of the background gas, which depends on the composition of the background gas.

Here, we make an approximate estimation by taking advantage of the previous investigations on the background gas inside the coated vapor cell. Previous work shows that the background gas in a paraffin-coated atomic vapor cell is mostly comprised of C3 (and higher) hydrocarbon molecules as well as hydrogen [37], and the typical value of the cross section for velocity-changing collisions is chosen as $\sigma_\mathrm{c} = 1\times 10^{-18}\,\mathrm{m}^2$ [38,69]. Thus, the pressure of the background gas in our coated cell could be approximately estimated as

$$p_\mathrm{b} = k_\mathrm{B}T/(\lambda\sigma_\mathrm{c}) \approx 1.70\,\mathrm{Pa}, \quad (28)$$

which is several orders of magnitude larger than the saturated vapor pressure of alkali atoms ($\sim 10^{-5}$ Pa). Consequently, the motion of atoms inside the coated cell is significantly suppressed by the background gas, which is shown phenomenally in Fig. 3(a). Based on Eqs. (17) and (25), the relation between the estimated pressure of background gas in the coated cell and the axial quadratic coefficient is shown in Fig. 3(b). As the background-gas pressure increases, the mean free path of alkali atoms could be suppressed to the order of millimeters

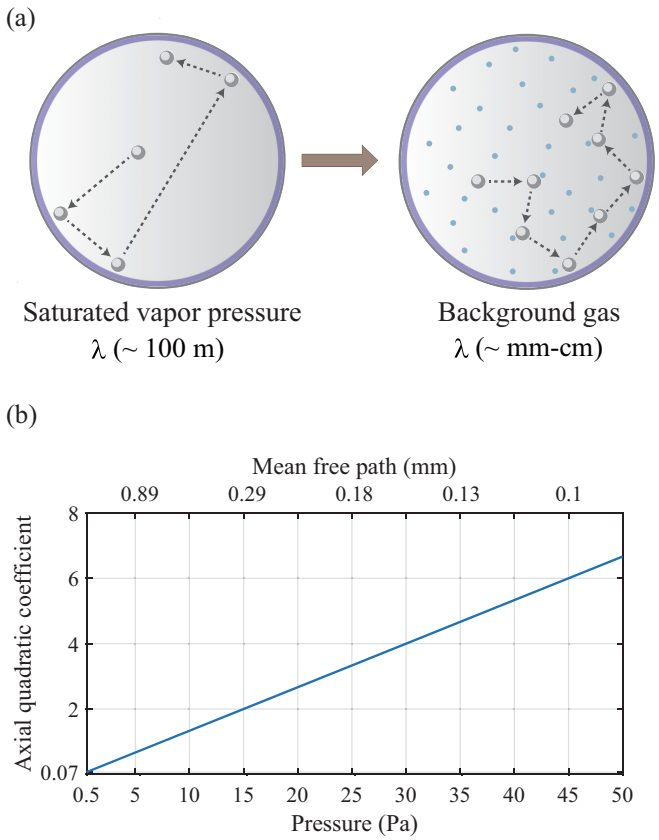

FIG. 3. (a) Background gas suppresses the mean free path of atoms inside the coated cell, from ~100 m at the saturated vapor pressure (left) to ~mm in the presence of background gas (right). The coating absorption effect is not shown in this figure. (b) Relation between the estimated pressure of background gas in our coated cell and the axial quadratic coefficient.

or even smaller, which results in a larger axial quadratic coefficient.

B. Evaluation of the number of bounces

The number of bounces N is the number of times that a polarized atom collides with the coating before depolarization, which is one of the core parameters used to characterize the performance of the antirelaxation coating. In general, N is estimated through measuring the longitudinal relaxation time T_1 [70].

For the coated cell with saturated alkali vapor pressure and without background gas, alkali atoms are in ballistic motion between adjacent wall collisions, and the number of bounces N is thus determined as

$$N = \frac{T_1}{T_{\text{wall}}} = \frac{T_1}{\frac{4R}{3}/\bar{v}}, \tag{29}$$

where T_{wall} is the average time between wall collisions [70–72], R is the radius of the cell, and $\bar{v}$ is the atomic velocity.

Considering the existence of background gas, atomic motion within the coated cell is modified from the ballistic regime to the intermediate regime, as is illustrated. It is thus natural to ask if it is still appropriate to use the ballistic-motion method shown in Eq. (29) to estimate the number of bounces in the coated cell with background gas.

Taking the potassium atomic cell coated with paraffin in our experiment as an example, the diffusion coefficient D and mean free path λ are estimated as $D \approx 0.2\,\text{m}^2/\text{s}$, $\lambda \approx 2.63\,\text{mm}$, and the average interval times for adjacent atom-atom collisions τ_λ and for diffusing across the cell τ_l are calculated as

$$\tau_\lambda \approx \frac{\lambda}{\bar{v}} \approx 5.8\,\mu\text{s}, \quad \tau_l \approx \frac{(4R/3)^2}{D} \approx 3.5\,\text{ms}, \tag{30}$$

where the radius of the cell is $R \approx 2\,\text{cm}$, the atomic velocity of a potassium atom is $\bar{v} \approx 453\,\text{m/s}$ at 50 °C, and T_1 is on the order of 10^{-1}–$10^0\,\text{s}$ for the cell that we use. We can find that $T_1 \gg \max[\tau_\lambda, \tau_l]$. Under this condition, as described in Ref. [73], the average of wall collisions N is shown as

$$\langle N \rangle = T_1 \left(\frac{l}{\bar{v}}\right)^{-1}, \tag{31}$$

where l represents the size of the boundary, and it could be evaluated as $\sim 4R/3$ for the spherical cell. It can be seen that Eq. (31) is equivalent to Eq. (29) for ballistic motion. The physical insight reveals that, due to the cluster of background gas near the inner surface of the cell, the alkali atoms tend to hit the wall several times before diffusing away from the wall, and for a long period T_1, the number of bounces corresponding to ballistic motion and diffusion will become similar. That is to say, when the relaxation time T_1 is much greater than the interval diffusion time τ_l, the model for ballistic motion shown in Eq. (29) can still be applied to estimate the number of bounces N for the coated cell with background gas.

When the pressure of background gas in the coated cell becomes larger, or if the cell is filled with high-pressure buffer gas, indicating that $T_1 \gg \max[\tau_\lambda, \tau_l]$ may not be satisfied, the number of bounces N can be estimated by the boundary condition for the diffusion equation of spin polarization [74], and the relation between T_1 and N has the form [75,76]

$$\frac{k}{\tan(kR)} = \frac{1}{R} - \frac{\bar{v}}{2N\left(2 - \frac{1}{N}\right)D},$$
$$\frac{1}{T_1} = Dk^2, \tag{32}$$

where k is the wave number of diffusion, and D is the diffusion coefficient. As a result, the number of bounces N could be solved numerically after measuring the longitudinal relaxation time T_1 experimentally.

It should be noted here that the presence of the background gas only alters the way to estimate the number of bounces between the polarized atoms with the wall under certain conditions. Whether the background gas could affect the performance of the coating or not is still under investigation.

V. CONCLUSIONS AND OUTLOOK

In this paper, we measure the spin polarization transverse relaxation caused by the first-order magnetic-field gradient in our paraffin-coated potassium vapor cell. The axial quadratic coefficient, which represents the relation between the linewidth of the magnetic resonance and the applied

gradient, $\partial B_{1z}/\partial z$, is measured to be over an order of magnitude larger than theoretical predictions. Such a deviation is caused by the occurrence of background gas. With the consideration of background gas in the coated cell, we propose a modified theoretical model that combines the Redfield theory with Langevin's diffusion model to analyze the magnetic-field-gradient-induced spin-relaxation effect. The result of our model is equal to that of the diffusion model in the diffusion regime, and it has the same form as the phase accumulation model in the ballistic regime. A specific theoretical expression is also provided for the intermediate regime. In addition, the mean free path of atoms in our coated cell estimated by our model is of the same order of magnitude as the pioneering works. Our work also provides a feasible method to determine the existence of the background gas, as well as an approximate estimation on the background gas pressure inside the coated cell without breaking the cell. In addition, our work can help to foster better comprehension about the performance of an antirelaxation coated cell by analyzing the magnetic-field-gradient-induced spin relaxation effect.

ACKNOWLEDGMENTS

We sincerely acknowledge the anonymous reviewer(s) for the insightful comments and constructive suggestions to make the descriptions and conclusions in the manuscript accurate and solid. This work is supported by the National Natural Science Foundation of China (Grant No. 62071012) and the National Hi-Tech Research and Development (863) Program. T.W. acknowledges the support from the start-up funding for young researchers of Peking University.

APPENDIX A: MEAN FREE PATH AND DIFFUSION COEFFICIENT

The mean free path represents the average distance traveled by an atom between successive atom-atom collisions. It is a classical physical concept that differs from the comprehensive relaxation mechanism about the coating. According to classical thermodynamics, the mean free path λ has the form

$$\lambda = \frac{k_B T}{\sqrt{2}\pi d^2 p}, \tag{A1}$$

where T is the temperature of atoms, k_B is the Boltzmann constant, d is the van der Waals diameter of atoms, and p is the pressure of the atomic system. Consider that the potassium atoms are at saturated vapor pressure, and the temperature of the atoms is assumed to be 50 °C. Under this condition, the pressure p_K and density n_K of potassium atoms are

$$p_K = 3.829 \times 10^{-5}\,\text{Pa},\ n_K = 8.588 \times 10^{15}\,\text{m}^{-3}, \tag{A2}$$

and the mean free path of the potassium atoms under this condition is derived as ~ 87 m and is a typical value for a coated cell without background gas.

Similarly, the definition of the diffusion coefficient comes from Fick's law in classical diffusion theory [29] and it characterizes the diffusion ability of atoms. For three-dimensional motion, it takes the form $D = \lambda\bar{v}/6$, where λ and $\bar{v}$ are the mean free path and thermal velocity of atoms, respectively.

APPENDIX B: LINEWIDTH AND RELAXATION TIME

For the M_x magnetometer system, the Bloch equation for describing the evolution of the spin polarization $\vec{M}$ in a rotating frame is

$$\frac{d\vec{M}}{dt} = \gamma\vec{M} \times \vec{B}_{\text{eff}} - \frac{M_x\vec{e}_x + M_y\vec{e}_y}{T_2} - \frac{(M_z - M_0)\vec{e}_z}{T_1}, \tag{B1}$$

where $\vec{B}_{\text{eff}} = (B_0 - \omega/\gamma)\vec{e}_z + B_{\text{RF}}\vec{e}_y$, ω is the frequency of an oscillating magnetic field B_{RF}, B_0 is a static bias magnetic field along the z-direction, and γ is the gyromagnetic ratio. M_0 refers to the spin polarization induced by optical pumping, and T_1 and T_2 are the longitudinal relaxation time and the transverse relaxation time, respectively.

The Bloch equation of spin polarization components in three directions over time is shown as

$$\begin{aligned}
\frac{dM_x}{dt} &= -\frac{M_x}{T_2} + (\gamma B_0 - \omega)M_y - \gamma B_{\text{RF}} M_z,\\
\frac{dM_y}{dt} &= -(\gamma B_0 - \omega)M_x - \frac{M_y}{T_2},\\
\frac{dM_z}{dt} &= \gamma B_{\text{RF}} M_x - \frac{M_z - M_0}{T_1}.
\end{aligned} \tag{B2}$$

The forms of the transverse polarization M_x and M_y in steady state are

$$\begin{aligned}
M_x &= -M_0 \frac{\omega_1 T_2}{1 + \Delta\omega^2 T_2^2 + \omega_1^2 T_1 T_2},\\
M_y &= M_0 \frac{\Delta\omega\omega_1 T_2^2}{1 + \Delta\omega^2 T_2^2 + \omega_1^2 T_1 T_2},
\end{aligned} \tag{B3}$$

where $\omega_1 = \gamma B_{\text{RF}}$, and $\omega_0 = \gamma B_0$, $\Delta\omega = \omega_0 - \omega$ is the frequency detuning. The expressions of M_x and M_y are Lorentz functions, which correspond to the in-phase and quadrature components of the magnetic resonance signal, respectively. If ω_1 meets with $\omega_1^2 T_1 T_2 \ll 1$, then the linewidth [full width at half-maximum (FWHM)] of the magnetic resonance signal is $\text{FWHM} = 2\Delta\omega/2\pi \approx 1/\pi T_2$, and the axial quadratic coefficient a_z between the magnetic-field gradient and the FWHM is

$$a_z = \text{FWHM}\left(\frac{\partial B_{1z}}{\partial z}\right)^{-2} = \frac{1}{\pi T_2}\left(\frac{\partial B_{1z}}{\partial z}\right)^{-2}. \tag{B4}$$

APPENDIX C: REDFIELD THEORY WITH TORREY'S DIFFUSION MODEL

McGregor applied the diffusion theory to describe the atomic motion in the cell [23],

$$\frac{\partial}{\partial t}\rho(\vec{r}, t \mid \vec{r}_0, t_0) = D\nabla^2\rho(\vec{r}, t \mid \vec{r}_0, t_0), \tag{C1}$$

where D is the diffusion coefficient. This equation is valid when the mean free path of the atoms is much smaller than the size of the cell ($\lambda \ll R$) [29,41]. The general solution for Eq. (C1) has the form

$$\begin{aligned}
\rho(\vec{r}, t \mid \vec{r}_0, t_0) = \frac{1}{R^3}\sum_{lmn} A_{ln} j_l\left(\frac{k_{ln}}{R}r\right) j_l\left(\frac{k_{ln}}{R}r_0\right)\\
\times Y_{lm}^*(\theta, \phi) Y_{lm}(\theta_0, \phi_0) \exp\left(-\frac{k_{ln}^2}{R^2} D|t - t_0|\right),
\end{aligned} \tag{C2}$$

under the boundary and initial conditions shown in Eqs. (9) and (10).

Combining Eqs. (C2) and (5), the complete expression of $\langle z(t)z(t+\tau)\rangle$ can be written as

$$\langle z(t)z(t+\tau)\rangle = R^2 \sum_n A_{1n}C_n \exp\frac{-k_{1n}^2 D|t-t_0|}{R^2}. \quad \text{(C3)}$$

Based on the Redfield method as mentioned in Eq. (1), the transverse relaxation information is obtained as

$$\frac{1}{\pi T_2} = \frac{1}{2\pi T_1} + \frac{\gamma^2}{2\pi} S_{1z}(0) \approx \frac{8\gamma^2 R^4}{175\pi D}\left(\frac{\partial B_{1z}}{\partial z}\right)^2, \quad \text{(C4)}$$

where we assume that $\nabla B_{1z} \approx \partial B_{1z}/\partial z$. Here, the longitudinal relaxation time T_1 is neglected under the condition of $\omega_0 R^2 \gg D$ [22],

$$\frac{1}{\pi T_1} \approx \frac{D}{\pi}\frac{|\nabla B_{1x}|^2 + |\nabla B_{1y}|^2}{B_0^2} \ll \frac{1}{\pi T_2}, \quad \text{(C5)}$$

where $\omega_0 = B_0\gamma$. This also means that when the static bias field B_0 is large enough, the impact of T_1 on T_2 can be ignored.

APPENDIX D: LANGEVIN'S DIFFUSION MODEL FOR THREE-DIMENSIONAL ATOMIC MOTION

According to Langevin's diffusion model for an unrestricted one-dimensional Brownian motion [29],

$$\langle (x(t)-x_0)^2\rangle = 2D\big[|t-t_0| - \tau_D\big(1-e^{-\frac{|t-t_0|}{\tau_D}}\big)\big], \quad \text{(D1)}$$

where $x(t)$ is the position of a particle at time t with initial position x_0, and $\langle\cdots\rangle$ denotes the ensemble average.

The conditional probability density $\rho(x,t \mid x_0,t_0)$ for a particle at position x at time t, with initial time t_0 and initial position x_0, has the form of a Gaussian function,

$$\rho(x,t \mid x_0,t_0) = \frac{\exp\big[-\frac{(x-x_0)^2}{2\langle[x(t)-x_0]^2\rangle}\big]}{\sqrt{2\pi\langle[x(t)-x_0]^2\rangle}} \quad \text{(D2)}$$

for unrestricted-one-dimensional motion. The relation between partial derivatives of $\rho(x,t \mid x_0,t_0)$ with respect to time and position is given by [5,29]

$$\frac{\partial}{\partial t}\rho(x,t \mid x_0,t_0) = D\big(1-e^{-\frac{|t-t_0|}{\tau_D}}\big)\frac{\partial^2\rho(x,t \mid x_0,t_0)}{\partial x^2}, \quad \text{(D3)}$$

which has the form of the Langevin equation in one-dimensional motion. The three-dimensional atomic motion in the coated cell described by Langevin's diffusion model is then shown as

$$\frac{\partial}{\partial t}\rho(\vec{r},t \mid \vec{r}_0,t_0) = D\big(1-e^{-\frac{|t-t_0|}{\tau_D}}\big)\nabla^2\rho(\vec{r},t \mid \vec{r}_0,t_0). \quad \text{(D4)}$$

APPENDIX E: NEUMANN BOUNDARY CONDITION

Based on classical kinetic theory, integrating incident velocities of different sizes and directions, we can get the flux of polarized atoms going to the coated wall with radius R [74],

$$J_+ = n_{\mathrm{K}}\left(\frac{\bar{v}\rho}{4} - \frac{D}{2}\frac{\partial\rho}{\partial n}\right)\Big|_{r=R}, \quad \text{(E1)}$$

and returning back from the wall,

$$J_- = n_{\mathrm{K}}\left(\frac{\bar{v}\rho}{4} + \frac{D}{2}\frac{\partial\rho}{\partial n}\right)\Big|_{r=R}, \quad \text{(E2)}$$

where n_{K} is the atomic density in the coated cell, ρ is the conditional probability density of atoms, and $\partial/\partial n$ means the normal derivative to the spherical wall.

If the number of bounces for the coating is N, then the probability of relaxation during a particular atom-wall collision is $1/N$. The reflected flux J_- also has the form

$$J_- = \left(1-\frac{1}{N}\right)J_+. \quad \text{(E3)}$$

Combining Eqs. (E1), (E2), and (E3), the boundary condition at the wall surface is [70]

$$\frac{\partial\rho}{\partial n}\Big|_{r=R} = -\frac{\bar{v}}{2N\big(2-\frac{1}{N}\big)D}\rho\Big|_{r=R}. \quad \text{(E4)}$$

If the number of bounces N is large enough, strictly speaking, $N \gg 1 + R/\lambda$, which means that the coated-wall-induced relaxation time is much longer than the motional time between adjacent wall collisions. Under this limit, the impact of wall relaxation can be ignored, and Eq. (E4) becomes the Neumann boundary condition [52,53]

$$\frac{\partial\rho}{\partial n}\Big|_{r=R} = 0. \quad \text{(E5)}$$

[1] N. Wilson, P. Light, A. Luiten, and C. Perrella, Ultrastable optical magnetometry, Phys. Rev. Appl. **11**, 044034 (2019).

[2] Y. Ding, W. Xiao, Y. Zhao, T. Wu, X. Peng, and H. Guo, Dual-species all-optical magnetometer based on a Cs-K hybrid vapor cell, Phys. Rev. Appl. **19**, 034066 (2023).

[3] R. Zhang, D. Kanta, A. Wickenbrock, H. Guo, and D. Budker, Heading-error-free optical atomic magnetometry in the Earth-field range, Phys. Rev. Lett. **130**, 153601 (2023).

[4] W. Chalupczak and R. M. Godun, Near-resonance spin-noise spectroscopy, Phys. Rev. A **83**, 032512 (2011).

[5] Y. Tang, Y. Wen, L. Cai, and K. Zhao, Spin-noise spectrum of hot vapor atoms in an anti-relaxation-coated cell, Phys. Rev. A **101**, 013821 (2020).

[6] Y. Wen, X. Li, G. Zhang, and K. Zhao, Zero-field spin-noise spectrum of an alkali vapor with strong spin-exchange coupling, Phys. Rev. A **104**, 063708 (2021).

[7] D. Budker, L. Hollberg, D. F. Jackson Kimball, J. Kitching, S. Pustelny, and V. V. Yashchuk, Microwave transitions and nonlinear magneto-optical rotation in anti-relaxation-coated cells, Phys. Rev. A **71**, 012903 (2005).

[8] E. P. Corsini, T. Karaulanov, M. Balabas, and D. Budker, Hyperfine frequency shift and Zeeman relaxation in alkali-metal-vapor cells with antirelaxation alkene coating, Phys. Rev. A **87**, 022901 (2013).

[9] S. Peck, N. Lane, D. Ang, and L. Hunter, Using tensor light shifts to measure and cancel a cell's quadrupolar frequency shift, Phys. Rev. A **93**, 023426 (2016).

[10] P. Bevington, R. Gartman, Y. V. Stadnik, and W. Chalupczak, Dual-frequency cesium spin maser, Phys. Rev. A **102**, 032804 (2020).

[11] D. F. Jackson, J. Dudley, Y. Li, D. Patel, and J. Valdez, Constraints on long-range spin-gravity and monopole-dipole couplings of the proton, Phys. Rev. D **96**, 075004 (2017).

[12] S. Afach *et al.*, Characterization of the global network of optical magnetometers to search for exotic physics (GNOME), Phys. Dark Universe **22**, 162 (2018).

[13] Z. Wang, X. Peng, R. Zhang, H. Luo, J. Li, Z. Xiong, S. Wang, and H. Guo, Single-species atomic comagnetometer based on ^{87}Rb atoms, Phys. Rev. Lett. **124**, 193002 (2020).

[14] V. Liberman and R. Knize, Relaxation of optically pumped Cs in wall-coated cells, Phys. Rev. A **34**, 5115 (1986).

[15] K. Nasyrov, S. Gozzini, A. Lucchesini, C. Marinelli, S. Gateva, S. Cartaleva, and L. Marmugi, Antirelaxation coatings in coherent spectroscopy: Theoretical investigation and experimental test, Phys. Rev. A **92**, 043803 (2015).

[16] C. P. Slichter, *Principles of Magnetic Resonance*, Springer Series in Solid-State Sciences (Springer, Heidelberg, 1990).

[17] R. Zhang, Y. Ding, Y. Yang, Z. Zheng, J. Chen, X. Peng, T. Wu, and H. Guo, Active magnetic-field stabilization with atomic magnetometer, Sensors **20**, 4241 (2020).

[18] Y. Ding, R. Zhang, J. Zheng, J. Chen, X. Peng, T. Wu, and H. Guo, Active stabilization of terrestrial magnetic field with potassium atomic magnetometer, Rev. Sci. Instrum. **93**, 015003 (2022).

[19] R. Zhang *et al.*, Recording brain activities in unshielded Earth's field with optically pumped atomic magnetometers, Sci. Adv. **6**, eaba8792 (2020).

[20] H. C. Torrey, Bloch equations with diffusion terms, Phys. Rev. **104**, 563 (1956).

[21] C. Neuman, Spin echo of spins diffusing in a bounded medium, J. Chem. Phys. **60**, 4508 (1974).

[22] G. Cates, S. Schaefer, and W. Happer, Relaxation of spins due to field inhomogeneities in gaseous samples at low magnetic fields and low pressures, Phys. Rev. A **37**, 2877 (1988).

[23] D. D. McGregor, Transverse relaxation of spin-polarized ^{3}He gas due to a magnetic-field gradient, Phys. Rev. A **41**, 2631 (1990).

[24] S. M. Clayton, Spin relaxation and linear-in-electric-field frequency shift in an arbitrary, time-independent magnetic field, J. Magn. Reson. **211**, 89 (2011).

[25] R. C. Wayne and R. M. Cotts, Nuclear-magnetic-resonance study of self-diffusion in a bounded medium, Phys. Rev. **151**, 264 (1966).

[26] A. Garroway and R. Cotts, NMR measurements of self-diffusion in lithium-ammonia and sodium-ammonia solutions, Phys. Rev. A **7**, 635 (1973).

[27] D. Sheng, A. Kabcenell, and M. V. Romalis, New classes of systematic effects in gas spin comagnetometers, Phys. Rev. Lett. **113**, 163002 (2014).

[28] X. Liu, C. Chen, T. Qu, K. Yang, and H. Luo, Transverse spin relaxation and diffusion-constant measurements of spin-polarized ^{129}Xe nuclei in the presence of a magnetic field gradient, Sci. Rep. **6**, 1 (2016).

[29] D. T. Gillespie and E. Seitaridou, *Simple Brownian Diffusion: An Introduction to the Standard Theoretical Models* (Oxford University Press, Oxford, 2013).

[30] S. Pustelny, D. F. Jackson Kimball, S. M. Rochester, V. V. Yashchuk, and D. Budker, Influence of magnetic-field inhomogeneity on nonlinear magneto-optical resonances, Phys. Rev. A **74**, 063406 (2006).

[31] M. Bouchiat and J. Brossel, Relaxation of optically pumped Rb atoms on paraffin-coated walls, Phys. Rev. **147**, 41 (1966).

[32] M. Stephens, R. Rhodes, and C. Wieman, Study of wall coatings for vapor-cell laser traps, J. Appl. Phys. **76**, 3479 (1994).

[33] J. Camparo, R. Frueholz, and B. Jaduszliwer, Alkali reactions with wall coating materials used in atomic resonance cells, J. Appl. Phys. **62**, 676 (1987).

[34] M. T. Graf *et al.*, Relaxation of atomic polarization in paraffin-coated cesium vapor cells, Phys. Rev. A **72**, 023401 (2005).

[35] Y. Yi, H. Robinson, S. Knappe, J. Maclennan, C. Jones, C. Zhu, N. Clark, and J. Kitching, Method for characterizing self-assembled monolayers as antirelaxation wall coatings for alkali vapor cells, J. Appl. Phys. **104**, 023534 (2008).

[36] S. N. Atutov, R. Calabrese, A. I. Plekhanov, and L. Tomassetti, Diffusion and photodesorption of molecular gases in a polymer organic film, Eur. Phys. J. D **68**, 6 (2014).

[37] A. Hatakeyama, T. Kuroda, N. Sekiguchi, and K. Ishikawa, Analysis of background gas in an alkali-metal vapor cell coated with paraffin, Appl. Phys. B **125**, 133 (2019).

[38] N. Sekiguchi and A. Hatakeyama, Non-negligible collisions of alkali atoms with background gas in buffer-gas-free cells coated with paraffin, Appl. Phys. B **122**, 81 (2016).

[39] S. Knappe and H. G. Robinson, Double-resonance lineshapes in a cell with wall coating and buffer gas, New J. Phys. **12**, 065021 (2010).

[40] A. Barabanov, R. Golub, and S. Lamoreaux, Electric dipole moment searches: Effect of linear electric field frequency shifts induced in confined gases, Phys. Rev. A **74**, 052115 (2006).

[41] R. Golub, R. M. Rohm, and C. Swank, Reexamination of relaxation of spins due to a magnetic field gradient: Identity of the Redfield and Torrey theories, Phys. Rev. A **83**, 023402 (2011).

[42] R. Golub and C. Swank, Relaxation, frequency shifts and other phenomena at the transition between diffusion and ballistic motion, arXiv:1012.4006v1 [cond-mat.stat.mech].

[43] J. M. Porrá, J. Masoliver, and G. H. Weiss, When the telegrapher's equation furnishes a better approximation to the transport equation than the diffusion approximation, Phys. Rev. E **55**, 7771 (1997).

[44] J. Masoliver, J. M. Porrá, and G. H. Weiss, Some two and three-dimensional persistent random walks, Physica A **193**, 469 (1993).

[45] C. Swank, A. Petukhov, and R. Golub, Correlation functions for restricted Brownian motion from the ballistic through to the diffusive regimes, Phys. Lett. A **376**, 2319 (2012).

[46] C. Swank, A. Petukhov, and R. Golub, Random walks with thermalizing collisions in bounded regions: Physical applications valid from the ballistic to diffusive regimes, Phys. Rev. A **93**, 062703 (2016).

[47] M. Guigue, G. Pignol, R. Golub, and A. Petukhov, Universality of spin relaxation for spin-1/2 particles diffusing over magnetic-field inhomogeneities in the adiabatic regime, Phys. Rev. A **90**, 013407 (2014).

[48] G. Pignol, M. Guigue, A. Petukhov, and R. Golub, Frequency shifts and relaxation rates for spin-1/2 particles moving in electromagnetic fields, Phys. Rev. A **92**, 053407 (2015).

[49] A. G. Redfield, On the theory of relaxation processes, IBM J. Res. Dev. **1**, 19 (1957).

[50] H. P. Breuer and F. Petruccione, *The Theory of Open Quantum Systems* (Oxford University Press on Demand, 2002).

[51] D. S. Lemons and A. Gythiel, Paul Langevin's 1908 paper On the Theory of Brownian Motion [sur la théorie du mouvement brownien], C. R. Acad. Sci. (Paris) **146**, 530 (1908)], Am. J. Phys. **65**, 1079 (1997).

[52] R. Shaham, O. Katz, and O. Firstenberg, Quantum dynamics of collective spin states in a thermal gas, Phys. Rev. A **102**, 012822 (2020).

[53] W. Happer, Y.-Y. Jau, and T. Walker, *Optically Pumped Atoms* (Wiley, Weinheim, 2010).

[54] S. Afach *et al.*, Gravitational depolarization of ultracold neutrons: Comparison with data, Phys. Rev. D **92**, 052008 (2015).

[55] D. Budker and D. F. Jackson Kimball, *Optical Magnetometry* (Cambridge University Press, Cambridge, 2013).

[56] K. Zhao and Z. Wu, Regionally specific hyperfine polarization of Rb atoms in the vicinity ($\sim 10^{-5}$ cm) of surfaces, Phys. Rev. A **71**, 012902 (2005).

[57] M. Schaden, K. Zhao, and Z. Wu, Effects of diffusion and surface interactions on the line shape of electron paramagnetic resonances in the presence of a magnetic field gradient, Phys. Rev. A **76**, 062502 (2007).

[58] E. Ulanski and Z. Wu, Measurement of dwell times of spin polarized rubidium atoms on octadecyltrichlorosilane-and paraffin-coated surfaces, Appl. Phys. Lett. **98**, 201115 (2011).

[59] Z. Wu, Wall interactions of spin-polarized atoms, Rev. Mod. Phys. **93**, 035006 (2021).

[60] S. Atutov and A. Plekhanov, Accurate measurement of the sticking time and sticking probability of Rb atoms on a polydimethylsiloxane coating, J. Exp. Theor. Phys. **120**, 1 (2015).

[61] K. Asakawa, Y. Tanaka, K. Uemura, N. Matsuzaka, K. Nishikawa, Y. Oguma, H. Usui, and A. Hatakeyama, Measurement of the temperature dependence of dwell time and spin relaxation probability of Rb atoms on paraffin surfaces using a beam-scattering method, Phys. Rev. A **104**, 063106 (2021).

[62] E. B. Alexandrov, M. V. Balabas, D. Budker, D. English, D. F. Kimball, C.-H. Li, and V. V. Yashchuk, Light-induced desorption of alkali-metal atoms from paraffin coating, Phys. Rev. A **66**, 042903 (2002).

[63] S. Gozzini and A. Lucchesini, Light-induced potassium desorption from polydimethylsiloxane film, Eur. Phys. J. D **28**, 157 (2004).

[64] S. Gozzini, A. Lucchesini, L. Marmugi, and G. Postorino, Light-induced sodium desorption from paraffin film, Eur. Phys. J. D **47**, 1 (2008).

[65] T. Karaulanov *et al.*, Controlling atomic vapor density in paraffin-coated cells using light-induced atomic desorption, Phys. Rev. A **79**, 012902 (2009).

[66] E. Breschi, G. Kazakov, C. Schori, G. Di Domenico, G. Mileti, A. Litvinov, and B. Matisov, Light effects in the atomic-motion-induced Ramsey narrowing of dark resonances in wall-coated cells, Phys. Rev. A **82**, 063810 (2010).

[67] H.-J. Lee and H. S. Moon, Ramsey effect of coherent population trapping in anti-relaxation-coated Rb vapor cells, J. Korean Phys. Soc. **63**, 890 (2013).

[68] M. Auzinsh, D. Budker, and S. Rochester, *Optically Polarized Atoms: Understanding Light-atom Interactions* (Oxford University Press, Oxford, 2010).

[69] C. G. Aminoff, J. Javanainen, and M. Kaivola, Collision effects in velocity-selective optical pumping of sodium, Phys. Rev. A **28**, 722 (1983).

[70] S. J. Seltzer, *Developments in Alkali-metal Atomic Magnetometry* (Princeton University Press, Princeton, NJ, 2008).

[71] S. N. Atutov, F. A. Benimetskiy, A. I. Plekhanov, V. A. Sorokin, and A. V. Yakovlev, Diffusion of Rb atoms in paraffin-coated resonant vapor cells, Eur. Phys. J. D **71**, 12 (2017).

[72] S. N. Atutov, A. I. Plekhanov, V. A. Sorokin, S. N. Bagayev, M. N. Skvortsov, and A. V. Taichenachev, Paraffin coated rubidium cell with an internal atomic vapor source, Eur. Phys. J. D **72**, 155 (2018).

[73] D. J. Bicout, E. I. Kats, A. K. Petukhov, and R. S. Whitney, Size independence of statistics for boundary collisions of random walks and its implications for spin-polarized gases, Phys. Rev. Lett. **110**, 010602 (2013).

[74] F. Masnou-Seeuws and M.-A. Bouchiat, Étude théorique de la relaxation d'atomes alcalins par collisions sur une paroi et sur un gaz, J. Phys. France **28**, 406 (1967).

[75] S. J. Seltzer, D. M. Rampulla, S. Rivillon-Amy, Y. J. Chabal, S. L. Bernasek, and M. V. Romalis, Testing the effect of surface coatings on alkali atom polarization lifetimes, J. Appl. Phys. **104**, 103116 (2008).

[76] S. J. Seltzer and M. V. Romalis, High-temperature alkali vapor cells with antirelaxation surface coatings, J. Appl. Phys. **106**, 114905 (2009).